

Database collecting in-plane test results of urm piers with bricks and blocks

Albanesi, Luca; Morandi, Paolo; Graziotti, Francesco; li Piani, Tiziano; Penna, Andrea; Magenes, Guido

Publication date

2018

Document Version

Final published version

Published in

Proceedings of the 16th European Conference on Earthquake Engineering

Citation (APA)

Albanesi, L., Morandi, P., Graziotti, F., li Piani, T., Penna, A., & Magenes, G. (2018). Database collecting in-plane test results of urm piers with bricks and blocks. In *Proceedings of the 16th European Conference on Earthquake Engineering: Thessaloniki, Greece*

Important note

To cite this publication, please use the final published version (if applicable).
Please check the document version above.

Copyright

Other than for strictly personal use, it is not permitted to download, forward or distribute the text or part of it, without the consent of the author(s) and/or copyright holder(s), unless the work is under an open content license such as Creative Commons.

Takedown policy

Please contact us and provide details if you believe this document breaches copyrights.
We will remove access to the work immediately and investigate your claim.

DATABASE COLLECTING IN-PLANE TEST RESULTS OF URM PIERS WITH BRICKS AND BLOCKS

Luca ALBANESI¹, Paolo MORANDI², Francesco GRAZIOTTI³, Tiziano LI PIANI⁴, Andrea PENNA⁵, Guido MAGENES⁶

ABSTRACT

In this paper, a database collecting the results of 188 in-plane cyclic tests on unreinforced masonry piers with bricks and blocks, constituted of different masonry materials, bed- and head-joint typologies, dimensions, boundary conditions, applied vertical loads and horizontal loading history, is presented.

The database, which will be freely shared, is organized in eight sections regarding general information and reference, information on masonry type, units and mortar, information on masonry walls, test conditions, estimated lateral resistances, experimental results of the cyclic tests, parameters of the bilinear curves and drift capacities.

A preliminary investigation on the in-plane displacement capacity of the walls is also proposed since it represents one of the main parameters to be used in the global seismic analyses for the design/assessment of masonry buildings. Particular attention has been dedicated to the evaluation of the displacement capacity at different limit states in relation with European codes.

Although the database, at the present stage, already contains several specimens, it will be continuously updated since this source of information of consistent and reliable test results represents a necessary step into the process of definition of shared rules in the European context, with particular reference to the definition of specific performance limit states and related capacity models for the in-plane seismic response of structural masonry walls.

Keywords: URM piers; bricks and blocks; in-plane cyclic tests; database; displacement capacity

1. INTRODUCTION

The development of a statistically significant database that assembles essential information and experimental results of in-plane cyclic tests on unreinforced masonry walls aims at the evaluation of the main parameters that may influence and govern the lateral response of URM buildings under seismic excitation, in order to improve the current analytical models and, possibly, to review code recommendations.

Attempts to build a systematic unified database with results of in-plane tests on masonry walls are already available in literature, for example the ones recently described by Augenti et al. (2012) and Gams et al. (2016), or the stone masonry database proposed by Vanin et al. (2017).

In this paper, a new database assorting the results of 188 in-plane cyclic tests on unreinforced single-leaf masonry piers carried out mainly in Europe within different research projects and found in literature has been developed. The database collects the results of tests on URM specimens constituted

¹ European Centre for Training and Research in Earthquake Engineering - EUCENTRE, Pavia, Italy, luca.albanesi@eucentre.it

² Department of Civil Engineering and Architecture - DICAr, University of Pavia, and EUCENTRE, Italy, paolo.morandi@unipv.it

³ DICAr, University of Pavia, and EUCENTRE, Italy, francesco.graziotti@unipv.it

⁴ Fac. of Civil Eng. and Geoscience, Structural Mechanics, TU Delft, The Netherlands, t.lipiani@tudelft.nl

⁵ DICAr, University of Pavia, and EUCENTRE, Italy, andrea.penna@unipv.it

⁶ DICAr, University of Pavia, and EUCENTRE, Italy, guido.magenes@unipv.it

of different masonry materials (with bricks and blocks), bed- and head-joint typologies, dimensions, boundary conditions, vertical applied loads and horizontal loading history, covering several failure modes.

Although the database already groups quite a lot of specimens, it will be continuously updated with other test results from new and past research, continuing to be freely shared. This reliable source of information of consistent test results represent a necessary step into the process of definition of shared rules in the European context, with particular reference to the definition of specific performance limit states and related capacity models for the in-plane seismic response of structural masonry walls.

A preliminary investigation on the in-plane displacement capacity of the walls is here proposed since it represents one of the main parameter to be used in the global seismic analyses for the design/assessment of masonry buildings.

2. DESCRIPTION OF THE DATABASE

All the considered in-plane cyclic shear tests were performed with an initial application of a vertical load and, consequently, through a cyclically acting horizontal load applied at the upper part of the wall, in order to simulate the conditions expected during an earthquake. The horizontal action was applied in the form of programmed displacements, cyclically imposed in both directions with step-wise increased amplitudes up to ultimate conditions of the specimens; at each displacement amplitude, the loading was repeated two or three times (this latter option for the majority of the tests). An example of a typical loading history and of an experimental test set-up is shown in Figure 1.

During each test, forces and displacements acting on the walls were measured and hysteresis loops recorded. The positive “+” direction is set, conventionally, when the forces and the displacements of the acquired Force-Displacement curves lie in the first quadrant and negative “-” when lie in the third quadrant.

In addition, in the majority of experimental campaigns, tests of characterization on units, mortar and masonry are also performed and thus the available results are reported in the database.

All the considered sources are listed in the references.

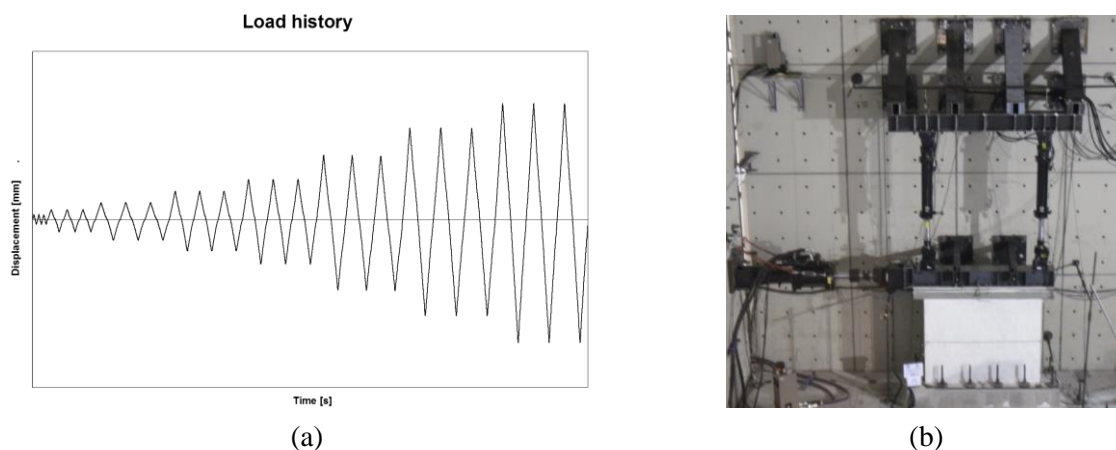


Figure 1. (a) Example of loading history in cyclic tests; (b) example of test set-up at the EUCENTRE of Pavia (Morandi et al. 2013).

The layout of the database is organized in eight sections with seventy-one columns of data, in addition to the first containing the sequential number of the specimens. The eight sections, whose number is reported in brackets, regard general information and reference [I], information on masonry type, units and mortar [II], information on masonry walls [III], test conditions [IV], calculated lateral resistances [V], experimental results through cyclic tests [VI], parameters of the bilinear curves [VII] and drift capacities [VIII].

All the data and parameters included in the different sections are summarized in Table 1; some of them are extracted directly from the sources while others are obtained by processing the available results or calculated according to code procedures. In the case of values or characteristics not available

or not obtainable through calculation, the sign “/” has been inserted in the cells.

Table 1: Parameters used in the database.

General info [I]	Source	Report, project, publication	Calculated resistances [V]	V_{shear} [kN]	$= V_{shear,min} \leq V_{shear,i} \leq V_{shear,max}$
	Specimen	Specimen name (original)		$V_{shear,lim,l}$ [kN]	Shear strength limit from EC6
Information on masonry type, units and mortar [II]	Material	Material of masonry unit	$V_{shear,lim,max}$ [kN]	Upper shear strength limit ($f_{v,lim} \cdot t \cdot l$)	
	l_u [mm]	Unit length	$V_{shear,lim}$ [kN]	$= \min(V_{shear,lim,i}; V_{shear,lim,max})$	
	w_u [mm]	Unit width	V_{pred} [kN]	$= \min(V_{flex}; V_{shear}; V_{shear,lim})$	
	h_u [mm]	Unit height	Expected failure	Expected failure mode	
	Void ratio [%]	Percentage of voids	Fail. mode	Observed failure mode	
	f_b [MPa]	Unit compressive strength	↓	Comparison between expected and test failure mode	
	d [-]	Shape factor	ξ range	Measure of dissipated energy	
	$f_{b,norm}$ [MPa]	Unit normalized compr. strength	δ_{cr} [mm]	Displ. at first crack	
	Bed-joints	Type of mortar bed-joints	$V_{max,exp}^+$ [kN]	Max pos. experimental force	
	Head-joints	Type of mortar head-joints	$V_{max,exp}^-$ [kN]	Max. neg. experimental force	
	Strength class	Mortar strength class	V_{pred}/V_{exp} [-]	Analytical/max. exp. force	
	f_m [MPa]	Mortar mean compr. strength	$\delta_{Vmax,exp}^+$ [mm]	Displ. at max. positive force	
Information on masonry walls [III]	l [m]	Wall length	$\delta_{Vmax,exp}^-$ [mm]	Displ. at min. positive force	
	t [m]	Wall thickness	$\delta_{max,f}^+$ [mm]	Max. pos. displ. at all completed cycles	
	h [m]	Wall height	$\delta_{max,f}^-$ [mm]	Max. neg. displ. at all completed cycles	
	h/l [-]	Wall height/length ratio	δ_{max}^+ [mm]	Max. positive displacement	
	n° of layers	Number of unit courses	δ_{max}^- [mm]	Max. negative displacement	
	G [MPa]	Masonry shear modulus	k_{el}^+ [kN/mm]	Stiffness in positive direction	
	E [MPa]	Masonry elastic modulus	k_{el}^- [kN/mm]	Stiffness in negative direction	
	f [MPa]	Masonry compressive strength	V_u^+ [kN]	Positive force of the plateau	
	f_{v0} [MPa]	Masonry initial shear strength	V_u^- [kN]	Negative force of the plateau	
	μ [-]	Masonry friction coefficient	δ_e^+ [mm]	Positive displacement at yield	
Test conditions [IV]	f_t [MPa]	Masonry diagonal tensile strength	δ_e^- [mm]	Negative displacement at yield	
	Boundary conditions	Test boundary conditions	δ_u^+ [mm]	Positive displ. at $0.8 \cdot V_u^+$	
	h_0/h [-]	Shear span ratio	δ_u^- [mm]	Negative displ. at $0.8 \cdot V_u^-$	
	σ_v [MPa]	Applied vertical stress	μ_u^+ [-]	δ_u^+/δ_e^+	
Calculated resistances [V]	σ_v/f [-]	Vert. stress/compr. strength ratio	μ_u^- [-]	δ_u^-/δ_e^-	
	M_u [kNm]	Resistant bending moment	μ [-]	$\text{Min}(\mu_u^+, \mu_u^-)$	
	$f_{v,lim}$ [MPa]	Shear strength limit from EC6	θ_{cr} [%]	Drift at first crack	
	V_{flex} [kN]	Shear strength at flexure	θ_e [%]	Drift at elastic limit	
	$V_{shear,i}$ [kN]	Shear strength from EC6	θ_{Vmax} [%]	Drift at peak force	
	$V_{shear,min}$ [kN]	Lower shear strength ($0.4 \cdot N$)	θ_u [%]	Drift at $0.8 \cdot V_u$	
	$V_{shear,max}$ [kN]	Upper shear strength ($f_{vd} \cdot t \cdot l$)	$\theta_{max,f}$ [%]	Max. drift at all completed cycles	
			θ_{max} [%]	Max. drift	
Information on masonry type, units and mortar [II]	Calculated resistances [V]	Experimental results (cyclic tests) [VI]	Parameters bilinear curves [VII]	Drift capacities [VIII]	

As described above, a total of 188 piers form the complete list, including 101 hollow clay with vertical perforation (HC), 11 lightweight aggregate concrete with vertical perforation (LAC), 18 solid unit calcium-silicate (CS), 26 solid unit autoclaved aerated concrete (AAC), 30 solid clay brick (SB-C) and 2 calcium-silicate brick (SB-CS) masonry piers, as reported in section [II] of the database. Figure 2 shows the composition of the database in terms of the masonry material of the tested specimens.

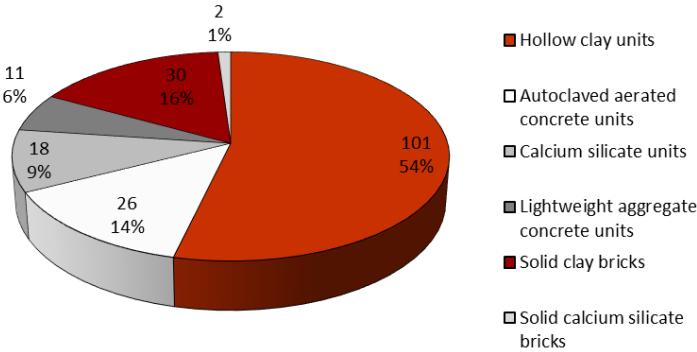


Figure 2. Masonry materials of the specimens included in the database.

The same section of the database, dedicated to information on units and mortar, reports information also about bed- and head-joints; general purpose (GP) or thin layer (TL) mortar bed-joints and different types of head-joints, such as completely filled (F), filled with thin layer mortar (TF), filled in the pocket (MP), unfilled with plain (U) or tongue and groove (UTG) units, characterize the masonry walls with blocks. The clay and calcium-silicate solid brick masonry is instead realized with general-purpose mortar. Figure 3 shows the head- and the bed-joint typologies for the tested masonry walls.

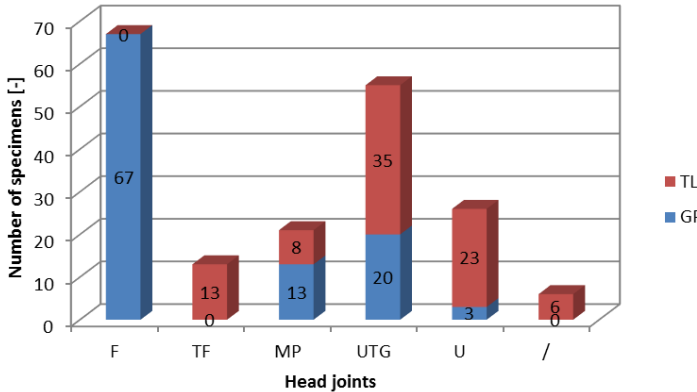


Figure 3. Head- and bed-joint typologies of the specimens included in the database.

The height of the piers, reported in section [III] of the database among other information about the masonry specimens, ranges from 1.17 m to 3.00 m, since only tests on walls with height larger than 1.15 m have been included in the database. More than 20 walls are characterized by heights lower or equal to 1.50 m (10 less or equal to 1.25 m) and therefore they were not considered in the analysis of the results, as explained in detail in chapter 3 of this paper, while the majority are included in the interval between 2.25 and 2.50 m.

The fourth section of the database reports the main information about the test conditions adopted for each specimen, such as the boundary conditions or the applied vertical load. Regarding the static scheme, the majority of the tests are conducted with “Double Fixed” (no rotation of the top beam, “DF”) and “Cantilever” (free rotation of the top beam, “C”) boundary conditions, with exception of few specimens that are performed with intermediate conditions, as reported in Figure 4.

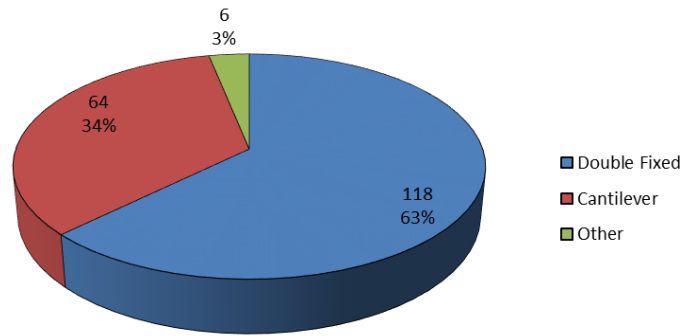


Figure 4. Composition of the database in terms of test boundary conditions.

As regards the vertical load applied to the wall during the test, it is interesting to evaluate the ratio σ_v/f , between the compression stress on the horizontal cross section of the wall (resulting from the applied vertical load) and the compressive strength of the masonry. Figure 5 reports the number of the specimens at given ranges of σ_v/f , showing that these ratios go from 2% to 41%, with the majority included between 2.5% and 22.5%.

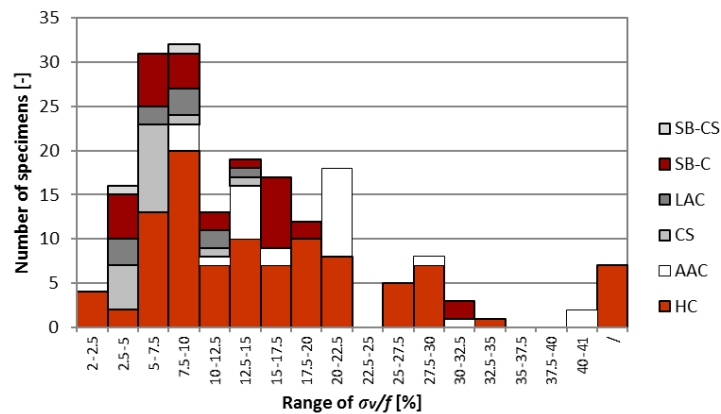


Figure 5. Number of the specimens at given intervals of σ_v/f ; “\” indicates the cases when the compression strength was not provided or evaluated.

The fifth section contains the calculation of the shear resistances of the specimens, starting from their geometrical and mechanical properties and according to the different code formulations proposed in Eurocode 6 (CEN 2005), aimed to the evaluation of the expected failure mode (by flexure or shear) for each test.

The failure modes actually obtained in the tests are instead reported in section [VI] of the database and cover several cases from flexural/rocking (F) to pure shear (S) with diagonal or step-wise cracking involving the joints and the units, sliding (SL) at the ends of the piers, “gaping” (G) with stepped cracking, and hybrid modes (H) with the occurrence of two different failure modes.

The failure modes identified in the available reports and papers have been carefully re-checked, for all the tests, according to the damage pattern of the specimens found in the pictures of the documents, the type of hysteretic curves and the values of the maximum attained displacement; sometimes, this interpretation has led to change the original evaluation of the mechanisms stated in the original reports and papers, in particular in the case of “hybrid” mechanisms, where the main involved modes have been now explicitly specified (for example, “H-FS” defines an hybrid mode with the occurrence of flexural and shear mechanisms).

The sixth section contains also all the other experimental results, distinguished for positive (+) and

negative (-) direction, such as the peak lateral force $V_{max,exp}^{+/-}$ obtained during the test and the corresponding displacements $\delta_{V_{max,exp}^{+/-}}$, the positive and negative maximum displacements of the last fully completed cycles $\delta_{max,f}^{+/-}$ (after two or three cycles, depending by the loading history) and the maximum displacements attained in the test in both directions $\delta_{max}^{+/-}$, independently by the full completion of all the cycles.

Section [VII] of the database is dedicated to the interpretation of the in-plane experimental response of the masonry walls; a common approach to evaluate the related seismic parameters is to idealize the cyclic envelope of the hysteresis loops by means of a bilinear curve. For all the tests, the approach described in Frumento et al. (2009), displayed in Figure 6, has consistently been used and the obtained parameters are included in this section of the database.

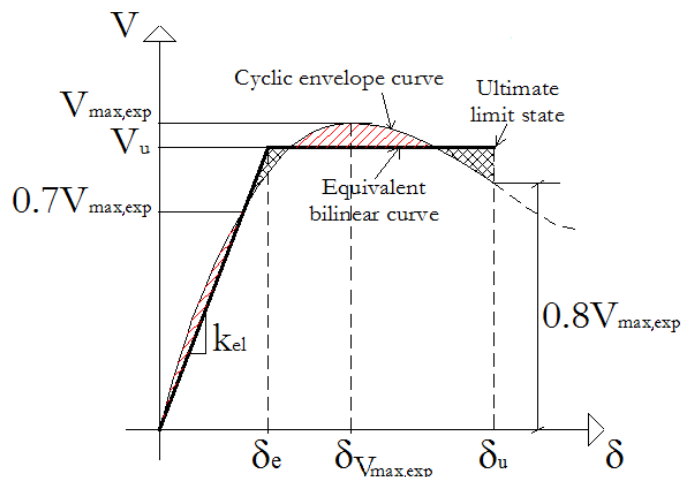


Figure 6. Idealization of the cyclic response: evaluation of the bi-linear curve from the hysteresis envelope.

Finally, the eighth section summarizes the main drift capacities identified for each specimen; the drift values are calculated dividing the horizontal displacements δ obtained from the tests by the height h of the specimens. With the exception of the drift at first crack θ_{cr} , the other relevant drift values (at the elastic limit θ_e , at peak force $\theta_{V_{max}}$, at 0.8 times the peak force θ_u , at the maximum displacement of the last fully completed cycle $\theta_{max,f}$, and at the maximum displacement θ_{max}) are estimated taking the minimum displacement between the positive and the negative directions.

3. ANALYSIS OF THE RESULTS

Wall specimens with very few courses of masonry units or very low heights can be subjected to the issue of a “size effect”, due to the higher influence of the boundary conditions, namely the confinement provided by the top and the bottom reinforced concrete or steel spreader beams, that can condition the results of the cyclic tests. In order to exclude this uncertain effect, only specimens with heights h larger or equal to 1.50 m and more than 7 courses have been considered in the following results. Therefore, the sample has been consequently limited to 135 piers (62 hollow clay, 26 aerated autoclaved concrete, 18 calcium silicate, 11 lightweight aggregate, 16 solid clay brick and 2 calcium-silicate solid brick masonry), out of the 188 of the original database.

Regarding the displacement capacity, the values of the experimental drift at peak force ($\theta_{V_{max}}$), the drift at 80% of V_{max} after the peak (θ_u) and at the maximum drift attained ($\theta_{max,f}$ and θ_{max}) have been plotted in Figures 7, 8 and 9 for all the considered specimens, divided by experimental failure mode.

The figures also show the drift limits imposed in the Italian norms for constructions (NTC 2008), in the latest draft of the Italian code (Draft of the New Technical Norms for Constructions 2014) and in part 3 of Eurocode 8 (EC8, CEN 2004), as summarized in Table 2, in relation with the different failure modes (shear and flexure) and with the limit states (Damage Limitation “DL”, Severe Damage “SD” and Near Collapse “NC” Limit States) defined in the Italian norms and in Eurocodes.

Table 2: Drift limits on URM piers in the considered European norms.

	Damage Limitation (DLLS) [%]	Severe Damage (SDLS) [%]		Near Collapse (NCLS) [%]	
		Flexure	Shear	Flexure	Shear
NTC 2008	0.3	0.8	0.4	-	-
New Draft Italian Norms	0.2	-	-	1.0	0.5
EC8-part 3	-	$0.8 \cdot h_0/l$	0.4	$1.07 \cdot h_0/l$	0.53

With the exception of two calcium-silicate specimens failing in pure flexure, the values of drift at peak force θ_{vmax} range in a rather limited interval between approximately 0.10% and 0.50% with a mean value of about 0.25%, independently by the masonry typologies and the final failure mode. These values of drift at peak force could be assumed as a reference value for the Damage Limitation Limit State (DLLS). NTC 2008 limits the drift at DLLS for URM buildings to 0.30%, whereas the latest draft of the Italian norms to 0.20%; no explicit limitation at DLLS for structural masonry buildings is instead present in EC8. As observable in Figures 7(a), 8(a) and 9(a), the drift limit at DLLS proposed in the new draft of the Italian norms appears to be appropriate.

On the other side, the values of drift θ_u , which are commonly related to the Life Safety/Severe Damage Limit State (SDLS), differ significantly as a function of the different experimental failure modes and masonry material. In particular, for pure shear failures, drifts between about 0.15% and 0.60% have been obtained, with mean values of 0.30% considering all the masonry typologies, 0.27% for hollow clay unit masonry, 0.37% for AAC masonry, 0.26% for calcium silicate masonry, 0.25% for lightweight aggregate concrete masonry (on only one specimen failing in shear) and 0.42% for clay solid brick masonry. Walls characterized by flexural/rocking mechanisms have instead provided much higher values of drift θ_u , with few cases below 0.70%; in the case of hollowed clay unit masonry, the mean value is equal to 1.0% whereas, for solid clay brick masonry, to 1.45%. For the other materials, few specimens have provided pure flexural mechanisms, in any case with values larger than 0.70%. Lastly, specimens with hybrid modes have obtained intermediate values of drift θ_u between pure shear and hybrid failure modes; the overall mean value of drift is settled around 0.70% and it is almost equal for all the materials, with the exception of the AAC masonry that provides lower levels of deformation capacity (0.38%). The current Italian norms (NTC 2008) limit the drift at SDLS for URM buildings to 0.40% in case of shear modes and to 0.80% for flexural modes, whereas the EC8 to 0.40% and to $0.80 \cdot h_0/l$ %, respectively. As evidenced by Figures 7(b) and 8(b), the drift limits at SDLS proposed in the Italian norms and in the EC8 seem to be safe-sided for flexural modes but in general overestimate the displacement capacity in the case of shear failures.

Similarly, the values of maximum drift capacity achieved at the end of the test $\theta_{max,f}$ and θ_{max} , which could be conservatively related to the Near Collapse Limit State (NCLS), differ significantly as a function of the masonry typologies and of the different failure modes. In fact, in the case of pure shear mechanisms, the overall mean value of θ_{max} is 0.41% ($\theta_{max} = 0.39%$ for HC, 0.45% for AAC, 0.39% for CS, 0.36% for LAC, 0.46% for SB-C), while, for flexural modes, the mean value of maximum drift is 1.35% for the hollow clay masonry, whereas it is approximately the same value of θ_u for solid clay brick masonry. Finally, the overall mean of drift θ_{max} for hybrid modes is 0.80%. Additionally, it is interesting to point out that for shear and hybrid modes, the difference between θ_{max} and $\theta_{max,f}$ is more significant than for the case of flexural modes; in the case of shear failures, the overall mean $\theta_{max,f}$ is 0.37% (with mean $\theta_{max} = 0.41%$) while, in the case of hybrid mechanism, is equal to 0.71% (mean $\theta_{max} = 0.80%$). The draft of the new Italian norms limits the drift at NCLS for URM buildings to 0.50% in case of shear modes and to 1.00% for flexural modes, whereas the EC8 to 0.53% and to $1.07 \cdot h_0/l$ %, respectively. As for SDLS, the drift limits for NCLS recommended in the EC8 and in the draft of the Italian norms provide safe-sided values for flexural modes but overestimate the displacement capacity in the case of shear failures, as shown in Figures 7(c) and 8(c).

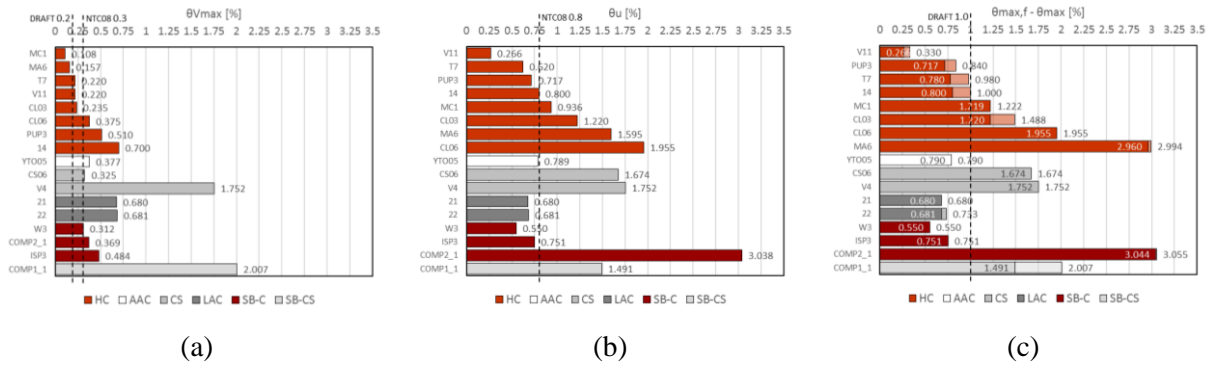


Figure 7. Experimental drift values for flexural/rocking mechanisms: at peak force θ_{Vmax} (a), at 80% of V_{max} after the peak θ_u (b), and at the maximum $\theta_{max,f}$ and θ_{max} (c) for different masonry materials. The limits for EC8 are not reported.

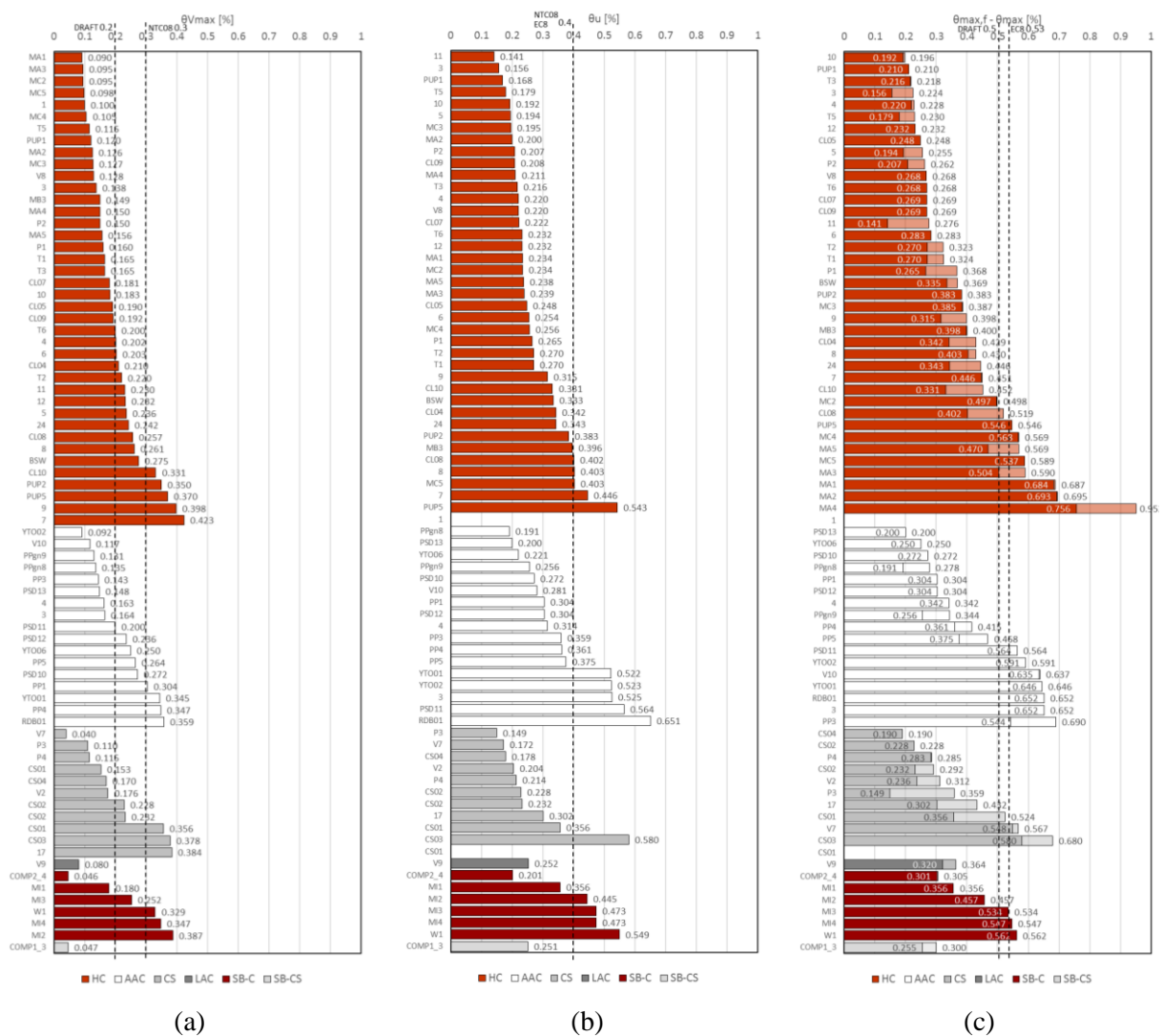


Figure 8. Experimental drift values for shear failures: at peak force θ_{Vmax} (a), at 80% of V_{max} after the peak θ_u (b), and at the maximum $\theta_{max,f}$ and θ_{max} (c) for different masonry materials.

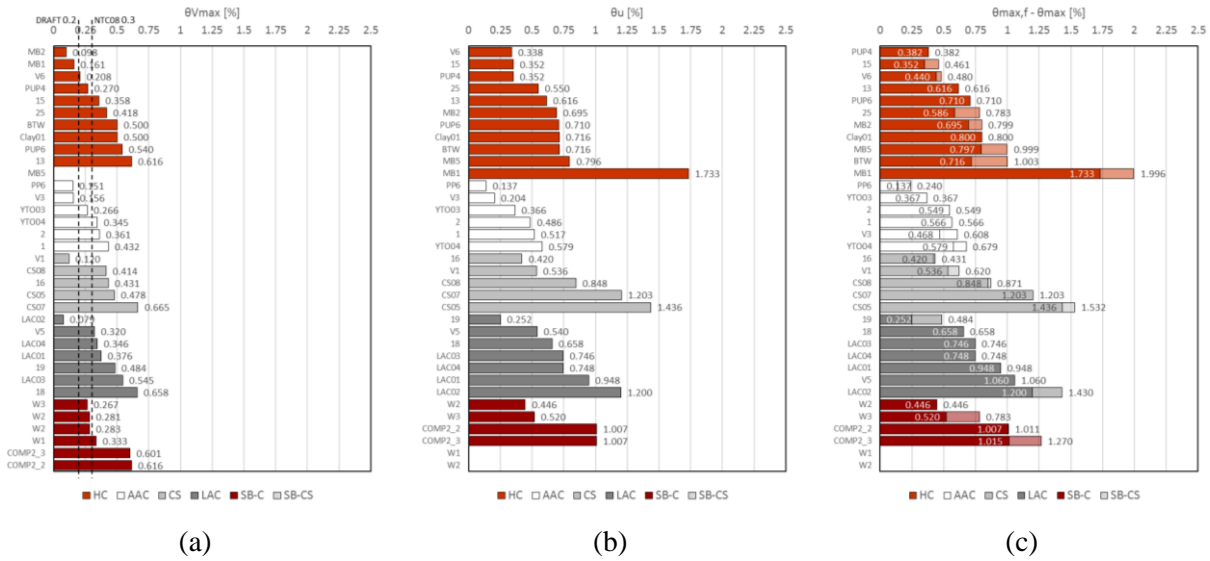


Figure 9. Experimental drift values for hybrid failures: at peak force $\theta_{V_{max}}$ (a), at 80% of V_{max} after the peak θ_u (b), and at the maximum $\theta_{max,f}$ and θ_{max} (c) for different masonry materials .

4. CONCLUSIONS

A database that assembles the information and the results of 188 in-plane cyclic tests carried out on unreinforced masonry piers with bricks and blocks, having different materials and typologies, dimensions, boundary conditions, vertical applied loads and horizontal loading history, has been developed and freely shared. The failure modes obtained in the tests cover a wide range of cases, from flexural/rocking to pure shear and hybrid modes with the occurrence of two different failure modes. It is important to underline that at this stage the largest effort has been devoted to the preparation of the database, which is intended to provide a continuously updated tool available for future studies aiming at the improvement of the understanding of the in-plane response of URM walls; the aspects here discussed concerning the displacement capacity only represent an introductory part of what can be obtained with the use of these data.

For the proposed preliminary interpretation of the test results, only specimens with heights $h \geq 1.50$ m and with more than 7 courses have been considered, in order to avoid “size effect” issues that can condition the results of the cyclic tests and influence a realistic evaluation of the effective failure modes and of the displacement capacity.

Regarding the deformation capacity at ultimate limit states (“Severe Damage” and “Near Collapse” Limit States), the results are found to be mainly influenced by the type of failure mode and by the masonry typology (and, within the same typology, in relation with other characteristics such as the head-joint types). In the case of pure shear, an overall mean value of drift θ_u equal to 0.30% has been obtained, with results varying as a function of different masonry typologies (i.e., 0.27% for hollow clay unit masonry, 0.42% for clay solid brick masonry) and reducing with higher compression stresses. Walls characterized by flexural/rocking mechanisms have instead provided much higher values of drift θ_u , with an average value of 1.15%, whereas in the case of hybrid modes, intermediate values of drift θ_u between the case of pure shear and flexural failure modes have been found (with an overall mean drift of about 0.70%). Similarly, the values of maximum drift capacity achieved at the end of the test θ_{max} differ significantly as a function of the masonry typologies and of the different failure modes attaining, in the case of pure shear mechanisms, an overall mean value of θ_{max} of 0.41%, whereas for flexural and hybrid modes of 1.34% and 0.80%, respectively.

Therefore, the drift limits at ultimate limit states reported in the Italian norms and in EC8 seem to be adequate for flexural modes but, in general, overestimate the displacement capacity in the case of shear failures.

5. ACKNOWLEDGMENTS

This research has been carried out at the University of Pavia and EUCENTRE and it has been partially funded by the Executive Project DPC-RELUIS 2013-2016 and by ASSOPLAN s.c.r.l.. The financial support received is gratefully acknowledged.

6. REFERENCES

- Abrams DP, Shah N (1992). Cyclic load testing of unreinforced masonry walls. U.S. Army Research Office.
- Anthoine A, Magonette G, Magenes G (1995). Shear-compression testing and analysis of brick masonry walls. *Proceedings of the 10th European Conference on Earthquake Engineering*, Vienna.
- Augenti N, Parisi F, Acconcia E (2012). MADA: online experimental database for mechanical modelling of existing masonry assemblages. *Proceedings of the 15th World Conference on Earthquake Engineering*, Lisbon.
- Bosiljkov V, Page A, Bokan-Bosiljkov V, Žarnić R (2003). Performance based studies of in-plane loaded unreinforced masonry walls. *Masonry International*, Vol. 16, No. 2, 39-50.
- Bosiljkov V, Tomazevic M (2004/2006). Optimization of shape of masonry units and technology of construction for earthquake resistant masonry buildings. *Research report* (part I and III), ZAG, Ljubljana.
- CEN (2005). Eurocode 6 - Design of masonry structures - Part 1-1: General rules for reinforced and unreinforced masonry structures. EN 1996-1-1:2005, European Committee for Standardisation, Brussels.
- CEN (2005). Eurocode 8 - Design of structures for earthquake resistance - Part 3: Assessment and retrofitting of buildings. EN 1998-3:2005, European Committee for Standardisation, Brussels.
- Costa A, Penna A, Magenes G (2011). Seismic performance of autoclaved aerated concrete (AAC) masonry: from experimental testing of the in-plane capacity of walls to building response simulation. *Journal of Earthquake Engineering*, Vol. 15, No. 1, 1-31.
- DM 14/01/2008. Norme Tecniche per le Costruzioni (NTC 2008). Gazzetta Ufficiale, n. 29 del 14/02/2008, Supplemento ordinario n.30.
- Draft of the New Technical Norms for Constructions. November 2014.
- Fehling E, Stuerz J, Emami A (2007). Test results on the behaviour of masonry under static (monotonic and cyclic) in plane lateral loads. *Deliverable D7.1a*, ESECMaSE Project, www.esecmase.org.
- Fehling E, Stürz J (2008). Experimentelle untersuchungen zum schubtragverhalten von porenbetonwandscheiben. *Report*, University of Kassel.
- Frumento S, Magenes G, Morandi P, Calvi GM (2009). Interpretation of experimental shear tests on clay brick masonry walls and evaluation of q-factors for seismic design. *Eucentre Research Report 2009/02*, IUSS Press, Pavia.
- Gams M, Triller P, Lutman M, Snoj J (2016). Seismic behaviour of URM walls: analysis of a database. *Proceedings of the 16th International Brick and Block Masonry Conference*, Padova.
- Graziotti F, Rossi A, Mandirola M, Penna A, Magenes G (2016). Experimental characterization of calcium-silicate brick masonry for seismic assessment. *Proceedings of the 16th International Brick and Block Masonry Conference*, Padova.
- Graziotti F, Tomassetti U, Rossi A, Marchesi B, Kallioras S, Mandirola M, Fragomeli A, Mellia E, Peloso S, Cuppari F, Guerrini G, Penna A, Magenes G (2016). Shaking table tests on a full-scale clay-brick masonry house representative of the Groningen building stock and related characterization tests. *Report EUC128/2016U*, Eucentre, Pavia.
- Magenes G, Calvi GM (1992). Cyclic behaviour of brick masonry walls. *Proceedings of the 10th World Conference on Earthquake Engineering*, Madrid.
- Magenes G, Morandi P, Penna A (2008). Test results on the behaviour of masonry under static cyclic in plane lateral loads. *Deliverable D7.1c*, ESECMaSE Project, www.esecmase.org.
- Manzouri T, Schuller MP, Shing PB, Amadei B (1995). Repair and retrofit of unreinforced masonry structures. *Earthquake Spectra*, Vol. 12, No. 4, 903-922.

- Modena C, Da Porto F, Garbin E (2005). Ricerca sperimentale sul comportamento di sistemi per muratura portante in zona sismica. *Report*, University of Padova.
- Morandi P, Albanesi L, Magenes G (2013). In-plane experimental response of masonry walls with thin shell and web clay units. *Proceedings of the Vienna Congress on Recent Advances in Earthquake Engineering and Structural Dynamics*, Vienna.
- Morandi P, Albanesi L, Magenes G (2014). URM walls with thin shell/web clay units and unfilled head-joints: cyclic in-plane tests. *Proceedings of the Second European Conference on Earthquake Engineering and Seismology*, Istanbul.
- Morandi P, Albanesi L, Magenes G (2015). Prestazioni sismiche di pannelli murari in blocchi di laterizio a setti sottili soggetti a test ciclici nel piano. *Atti del XVI Convegno ANIDIS - L'ingegneria Sismica in Italia*, L'Aquila.
- Ötes A, Löring S (2003). Tastversuche zur identifizierung des verhaltensfaktors von mauerwerksbauten für den erdbebennachweis. *Technical report*, University of Dortmund.
- Penna A, Mandirola M, Rota M, Magenes G (2015). Experimental assessment of the in-plane lateral capacity of autoclaved aerated concrete (AAC) masonry walls with flat-truss bed-joint reinforcement. *Construction and Building Materials*, Vol. 82, 155-166.
- Petry S, Beyer K (2014). Influence of boundary conditions and size effect on the drift capacity of URM walls. *Engineering structures*, Vol. 65, 76-88.
- Rosti A, Penna A, Rota M, Magenes G (2016). In-plane cyclic response of low-density AAC URM walls. *Material and Structures*, Vol. 49, No. 11, 4785-4798.
- Salmanpour AH, Mojsilović N, Schwartz J (2015). Displacement capacity of contemporary unreinforced masonry walls: an experimental study. *Engineering Structures*, Vol. 89, 1-16.
- Vanin F, Zaganelli D, Penna A, Beyer K (2017). Estimates for the stiffness, strength and drift capacity of stone masonry walls based on 123 quasi-static cyclic tests reported in the literature. *Bulletin of Earthquake Engineering*, Vol. 15, No. 12, 5435-5479.
- Zilch K, Finck W, Grabowski S, Schermer D, Scheufler W (2008). Test results on the behaviour of masonry under static cyclic in plane lateral loads. *Deliverable D7.1.b*, ESECMaSE Project, www.esecmase.org.